

CONFIGURATION ANALYSIS OF A TORQUELESS HELICOPTER CONCEPT

Theo van Holten, Monique Heiligers
Delft University of Technology, Faculty of Aerospace Engineering

Keywords: *Helicopter, Ornicopter, Vibrations, Rotor lay-out, Reaction torque*

Abstract

The Ornicopter is a single rotor helicopter without reaction torque. This is achieved by forced flapping of the blades. To investigate the resulting vibrations due to the forced flapping the expressions for the forces and moments that act about the rotor hub will be derived. Expressions for the forced flapping moment, the flapping angle and the flapping power will be derived as well.

Based on these expressions three different Ornicopter rotor concepts will be analyzed: the double teeter, the 2x2 anti-symmetrical and the three bladed 1-plane configuration. The 2x2 anti-symmetrical configuration yields the most favorable vibration results.

1 Notations

Restricted to those not defined in the text or in the figures:

c_{l_α}	Derivative of the lift coefficient for a blade element w.r.t. the angle of attack
C_{l_α}	Derivative of the lift coefficient w.r.t. the angle of attack
dD_p	Profile drag on a blade element
I	Moment of inertia of the blade w.r.t. the flapping hinge
dL	Lift on a blade element
R	Rotor radius
α	Angle of attack
β	Flapping angle
θ	Pitch angle
ψ	Azimuth angle

ρ Air density

Ω Angular speed of the rotor

2 General introduction

The engine torque supplied to a conventional helicopter rotor necessitates complex and costly anti-torque devices - such as tailrotors - to prevent spinning of the fuselage. During previous research [1][2] it has been demonstrated that the Ornicopter is a single rotor helicopter without reaction torque, and therefore does not need an anti-torque device.

To achieve this torqueless situation, the rotor blades of the Ornicopter will be forced to flap up and down, a motion that might cause severe vibrations in the forces and moments that act about the rotor hub. In this paper expressions for these forces and moments will be derived, and it will be shown that most of the vibrations can be cancelled out by choosing an appropriate number of blades and flapping sequence of the blades.

3 Design formulas for the Ornicopter

First some expressions for the essential, basic Ornicopter quantities will be derived: the mechanical flapping moment (i.e. the moment applied by the mechanical flapping mechanism to the Ornicopter blade), the flapping angle and the mechanical flapping power. These expressions will subsequently be used to derive expressions for all six dynamic fluctuating force and moment components about the rotor hub as these are caused by one rotor blade. Finally it will be indicated in what way the forces and

moments that occur due to all rotor blades (the entire rotor) can be calculated from the expressions for the forces and moments as they are caused by one single rotor blade.

3.1 Mechanical flapping moment, flapping angle and mechanical flapping power

An expression for the mechanical flapping power (P_{fl}) has been derived in the accompanying paper [2] and is repeated below:

$$0 = P_i + P_p - \frac{1}{2\pi} \int_0^{2\pi} (M_{fl} - I\Omega^2 \beta_0) \dot{\beta} d\psi \quad (1)$$

$$0 = P_i + P_p - P_{fl} \quad (2)$$

$$P_{fl} = \frac{1}{2\pi} \int_0^{2\pi} (M_{fl} - I\Omega^2 \beta_0) \dot{\beta} d\psi \quad (3)$$

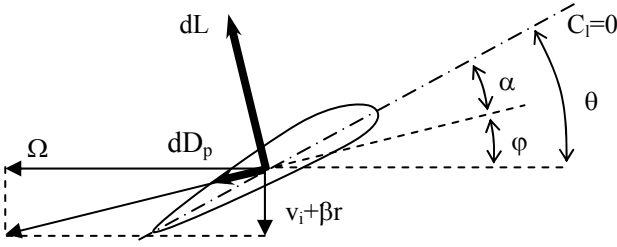


Fig. 1: Aerodynamic forces and velocities on a blade element at distance r from the rotor hub

Equation (1) in combination with the equation of motion and its solution as derived in the accompanying paper [2]:

$$\ddot{\beta} + \Omega^2 \beta = \frac{M_a}{I} + \frac{M_{fl}}{I} \quad (4)$$

$$M_a = -M_{fl} + I\Omega^2 \beta_0 \quad (5)$$

can be used to find an expression for the mechanical flapping moment M_{fl} and the flapping angle β . In order to do so, the aerodynamic moment is expressed as (see also figure 1):

$$M_a = \int_0^R c_{l\alpha} \alpha \frac{1}{2} \rho (\Omega r)^2 c r dr \quad (6)$$

$$M_a = \frac{1}{2} \frac{\rho C_{l\alpha} c R^4}{I} I \Omega^2 \int_0^1 \left(\theta - \frac{\lambda_i}{x} - \beta' \right) x^3 dx \quad (7)$$

$$M_a = \int_0^R c_{l\alpha} \left[\theta - \frac{v_i}{\Omega r} - \beta' \right] \frac{1}{2} \rho (\Omega r)^2 c r dr \quad (8)$$

$$M_a = \frac{\gamma}{2} I \Omega^2 \left(\frac{\theta}{4} - \frac{\lambda_i}{3} - \frac{\beta'}{4} \right) \quad (9)$$

with x the non-dimensional rotor radius, γ the Lock number, β' the derivative of the flap angle w.r.t. the azimuth angle and λ_i the non-dimensional induced velocity defined as:

$$x = \frac{r}{R} \quad (10)$$

$$\gamma = \frac{\rho C_{l\alpha} c R^4}{I} \quad (11)$$

$$\beta' = \frac{d\beta}{d\psi} = \frac{d\beta}{d\Omega t} = \frac{\dot{\beta}}{\Omega} \quad (12)$$

$$\lambda_i = \frac{v_i}{\Omega r} \quad (13)$$

If the non-dimensional aerodynamic flapping moment (m_a) and the non-dimensional mechanical flapping moment (m_{fl}) are defined by:

$$m_a = \frac{M_a}{\Omega^2 I} \quad (14)$$

$$m_{fl} = \frac{M_{fl}}{\Omega^2 I} \quad (15)$$

then, using equations (9), (14) and (15) equation (5) can be written as:

$$m_{fl} = -\frac{\gamma}{2} \left(\frac{\theta}{4} - \frac{\lambda_i}{3} - \frac{\beta'}{4} \right) + \beta_0 \quad (16)$$

Now assume that:

$$m_{fl} = A \cos \psi + B \sin \psi \quad (17)$$

$$\beta = \beta_0 + C \cos \psi + S \sin \psi \quad (18)$$

Substitution of these equations into (16) gives:

$$A \cos \psi + B \sin \psi = -\frac{\gamma}{8} \theta + \frac{\gamma}{6} \lambda_i + \frac{\gamma}{8} (-C \sin \psi + S \cos \psi) + \beta_0 \quad (19)$$

It can now be seen that:

$$A = \frac{\gamma}{8} S \quad (20)$$

$$B = -\frac{\gamma}{8} C \quad (21)$$

Thus, the non-dimensional mechanical flapping moment as a function of the flapping coefficients is given by:

$$m_{fl} = \frac{\gamma}{8} S \cos \psi - \frac{\gamma}{8} C \sin \psi \quad (22)$$

By combining equations (17), (18), (20) and (21) a relation can be found between the maximum flapping angle (β_{\max}) and the maximum non-dimensional flapping moment ($m_{fl_{\max}}$):

$$m_{fl_{\max}} = \sqrt{A^2 + B^2} = \frac{\gamma}{8} \beta_{\max} \quad (23)$$

The final step is to substitute equations (17), (18) and (23) into the expression for the flapping power (3):

$$P_{fl} = \frac{I\Omega^3}{2} \frac{\gamma}{8} \beta_{\max}^2 = \frac{I\Omega^3}{2} \frac{8}{\gamma} m_{fl_{\max}}^2 \quad (24)$$

Recapitulating, since P_i and P_p can be calculated, equation (2) gives an expression for the flapping power P_{fl} . Once P_{fl} is known, equation (24) can be used to calculate the maximum flapping angle and maximum non-dimensional flapping moment.

3.2 Moments and forces on the rotor hub

The expressions for the flapping power, mechanical flapping moment and flapping angle

can now be used to derive the forces and moments as these are caused by each rotor blade about the rotor hub. The expressions that will be derived in this section are valid for one single rigid rotor blade with a central flapping hinge during hover.

3.2.1 Roll moment and pitch moment

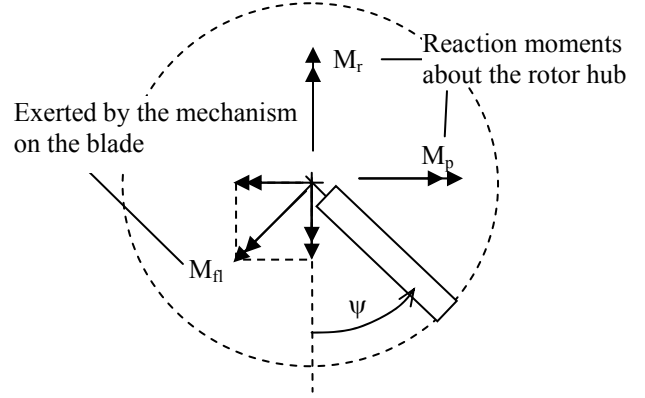


Fig. 2: Pitch and roll moment about the rotor hub due to the mechanical flapping moment

Using figure 2 and equations (15), (18), (20) and (21) the expressions for the non-dimensional roll moment (m_r) and non-dimensional pitch moment (m_p) about the rotor hub caused by one single rotor blade are:

$$m_r = \frac{M_r}{I\Omega^2} = \frac{M_{fl}}{I\Omega^2} \sin \psi \quad (25)$$

$$m_r = -\frac{\gamma}{16} C + \frac{\gamma}{16} (S \sin 2\psi + C \cos 2\psi) \quad (26)$$

$$m_p = \frac{M_p}{I\Omega^2} = \frac{M_{fl}}{I\Omega^2} \cos \psi \quad (27)$$

$$m_p = \frac{\gamma}{16} S + \frac{\gamma}{16} (S \cos 2\psi - C \sin 2\psi) \quad (28)$$

3.2.2 Torque

Looking at figure 3 the torque (dQ) that is caused by a blade element at distance r from the rotor hub can be expressed as (assuming small angles):

$$dQ = -2\Omega^2 \beta' \beta r^2 dm + dL \phi r + dD_p r \quad (29)$$

Expressions for the lift, profile drag and inflow angle will be given below and will subsequently be substituted into equation (29). The lift on a blade element is given by (see also figure 1):

$$dL = c_{l\alpha} \left[\theta - \frac{\lambda_i R}{r} - \beta' \right] \frac{1}{2} \rho (\Omega r)^2 c dr \quad (30)$$

$$dL = \frac{\gamma}{2} \frac{\Omega^2 I}{R} \left[\theta - \frac{\lambda_i}{x} - \beta' \right] x^2 dx \quad (31)$$

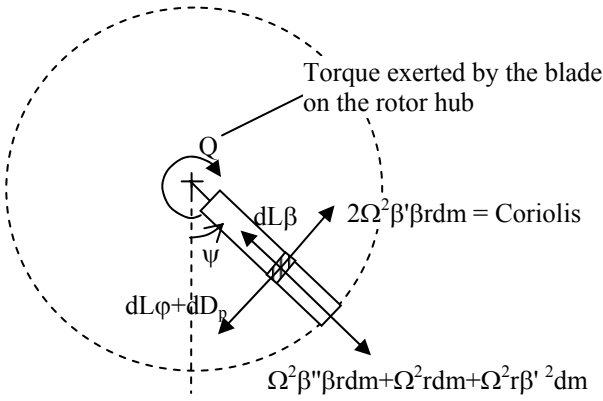


Fig. 3: Top view of the forces acting on a blade element (including inertia forces) at a distance r from the rotor hub.

The profile drag on a blade element is given by:

$$dD_p = c_{dp} \frac{1}{2} \rho (\Omega r)^2 c dr \quad (32)$$

$$dD_p = c_{dp} \frac{1}{2} \rho \Omega^2 R^3 x^2 c dx \quad (33)$$

And the inflow angle φ is given by:

$$\varphi = \frac{v_i + \dot{\beta}r}{\Omega r} = \frac{\lambda_i \Omega R + \beta' \Omega r}{\Omega r} = \frac{\lambda_i}{x} + \beta' \quad (34)$$

Substitution of the above equations in equation (29) yields the resulting torque per blade element:

$$\begin{aligned} dQ = & -2\Omega^2 \beta' \beta r^2 dm + \\ & + \frac{\gamma}{2} \Omega^2 I \left[\theta - \frac{\lambda_i}{x} - \beta' \right] \left[\frac{\lambda_i}{x} + \beta' \right] x^3 dx + \\ & + c_{dp} \frac{1}{2} \rho \Omega^2 R^4 x^3 c dx \end{aligned} \quad (35)$$

Integration and conversion to the non-dimensional torque (q) gives:

$$\begin{aligned} q = & \frac{Q}{I\Omega^2} = -2\beta'\beta + \\ & + \frac{\gamma}{2} \left[-\frac{\beta'^2}{4} + \beta' \left(\frac{\theta}{4} - \frac{2\lambda_i}{3} \right) + \lambda_i \left(\frac{\theta}{3} - \frac{\lambda_i}{2} \right) \right] + \\ & + \bar{C}_{dp} \frac{\rho R^4 c}{8I} \end{aligned} \quad (36)$$

Substitution of equation (18) (and its derivatives) into (36) yields:

$$\begin{aligned} q = & \bar{q} - 2\beta_0 [-C \sin \psi + S \cos \psi] + \\ & + \sin 2\psi \left[\gamma \frac{CS}{8} - (S^2 - C^2) \right] + \\ & - \cos 2\psi \left[2SC + \gamma \frac{S^2 - C^2}{16} \right] + \\ & + \frac{\gamma}{2} (-C \sin \psi + S \cos \psi) \left(\frac{\theta}{4} - \frac{2\lambda_i}{3} \right) \end{aligned} \quad (37)$$

With the non-dimensional torque \bar{q} given by:

$$\begin{aligned} \bar{q} = & -\frac{\gamma}{16} \beta_{\max}^2 + \bar{C}_{dp} \frac{\rho R^4 c}{8I} + \\ & + \frac{\gamma}{2} \lambda_i \left(\frac{\theta}{3} - \frac{\lambda_i}{2} \right) \end{aligned} \quad (38)$$

3.2.3 Vertical force

The resulting vertical force (dV) on the hub caused by a blade element is derived using figure 4. Assuming small angles, the following expression results:

$$dV = dL - \Omega^2 \beta'' r dm \quad (39)$$

Using the relation for the lift as in equation (30) it is calculated that:

$$V = \int_0^1 \frac{\gamma}{2} \frac{\Omega^2 I}{R} \left[\theta - \frac{\lambda_i}{x} - \beta' \right] x^2 dx - \Omega^2 \beta'' \int r dm \quad (40)$$

$$V = \frac{\gamma}{2} \frac{\Omega^2 I}{R} \left[\frac{\theta}{3} - \frac{\lambda_i}{2} - \frac{\beta'}{3} \right] - \Omega^2 \beta'' S_{bl} \quad (41)$$

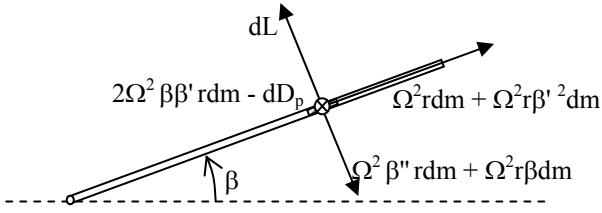


Fig. 4: Side view of the forces acting on a blade element (including inertia forces) at a distance r from the rotor hub.

In which S_{bl} is the first moment of the blade about the flapping hinge. Using the expressions for the flapping angle and converting to the non-dimensional vertical force (v) it is derived that:

$$v = \frac{V}{I\Omega^2} R = \bar{v} - \frac{\gamma}{2} \left[\frac{-C \sin \psi + S \cos \psi}{3} \right] + \frac{S_{bl} I}{R} [C \cos \psi + S \sin \psi] \quad (42)$$

In which the average non-dimensional vertical force (\bar{v}) is given by:

$$\bar{v} = \frac{\gamma}{2} \left[\frac{\theta}{3} - \frac{\lambda_i}{2} \right] \quad (43)$$

3.2.4 In-plane forces

The radial in-plane force (dF_R) caused by a blade element on the rotor hub can, using figure 5, be expressed as:

$$dF_R = dL\beta - \Omega^2 \beta'' \beta r dm + \Omega^2 r dm - \Omega^2 r \beta'^2 dm \quad (44)$$

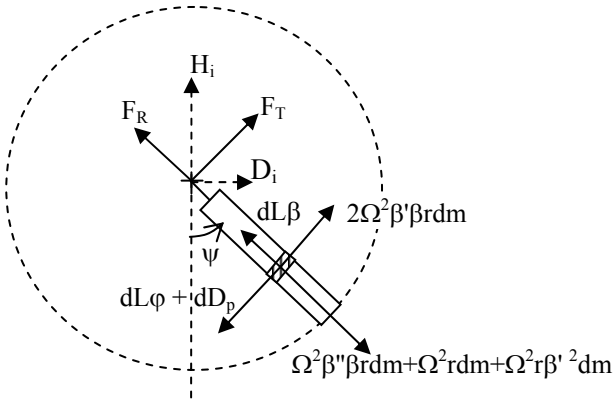


Fig. 5: Top view of the forces acting on a blade element (including inertia forces)

Using the relation for the lift as given by equation (31), and integrating yields for the non-dimensional radial force (f_R):

$$f_R = \frac{F_R R}{I\Omega^2} = \frac{\gamma}{2} \beta \left[\frac{\theta}{3} - \frac{\lambda_i}{2} \right] - \frac{\gamma}{6} \beta \beta' + \frac{R}{I} S_{bl} [\beta'' \beta + 1 + \beta'^2] \quad (45)$$

The tangential component (dF_T) of the force acting on the rotor hub caused by a blade element can be derived the same way, looking at figure 5:

$$dF_T = 2\Omega^2 \beta \beta' r dm - dL \phi - dD_p \quad (46)$$

Substitution of equations (31) and (33), and integrating gives for the non-dimensional tangential force f_T :

$$f_T = \frac{F_T R}{I\Omega^2} = \frac{S_{bl} R}{I} 2\beta \beta' + \frac{\gamma}{2} \left[\lambda_i \left(\frac{\theta}{2} - \lambda_i \right) + \beta' \left(\frac{\theta}{3} - \lambda_i \right) - \frac{\beta'^2}{3} \right] - \frac{\gamma \bar{C}_{Dp}}{6 C_{l\alpha}} \quad (47)$$

Instead of expressing the in-plane forces on the hub in a radial and tangential component, it is also possible to express them in a H_i and D_i component, in the longitudinal and lateral direction respectively (see figure 5). The non-dimensional H_i force component on the rotor hub (h_i) is calculated as:

$$h_i = \frac{H_i R}{I\Omega^2} = f_R \cos \psi + f_T \sin \psi \quad (48)$$

By substitution of equations (45) and (47) the average h_i force (\bar{h}_i) can be obtained from equation (48), and is given by the following expression:

$$\bar{h}_i = \frac{\gamma C}{4} \left[\frac{\theta}{3} - \frac{\lambda_i}{2} \right] + \frac{\gamma C}{4} \left(\frac{\theta}{3} - \lambda_i \right) - \frac{\gamma}{12} S \beta_0 - \frac{S_{bl} R C \beta_0}{I} \frac{1}{2} \quad (49)$$

The fluctuating part of the h_i force (Δh_i) is also derived from equation (48) and, after some calculation, given by:

$$\begin{aligned} \Delta h_i = & \left\{ \frac{\gamma}{2} \left(\frac{\theta}{3} - \frac{\lambda_i}{2} \right) \beta_0 - \frac{\gamma}{6} CS - \frac{S_{bl}R}{I} \right\} \cos \psi + \\ & + \left\{ \frac{\gamma}{6} C^2 - \frac{\gamma}{2} \lambda_i \left(\frac{\theta}{2} - \lambda_i \right) - \frac{1}{6} \frac{\bar{C}_{Dp} \rho R^4 c}{I} \right\} \sin \psi + \\ & \left\{ \frac{\gamma}{2} \left(\frac{\theta}{3} - \frac{\lambda_i}{2} \right) \frac{C}{2} - \frac{\gamma}{6} \frac{S \beta_0}{2} + \right. \\ & + \left. \frac{S_{bl}R}{I} \frac{3C\beta_0}{2} - \frac{\gamma}{2} \left(\frac{\theta}{3} - \lambda_i \right) \frac{C}{2} \right\} \cos 2\psi + \\ & + \left\{ \frac{\gamma}{2} \left(\frac{\theta}{3} - \frac{\lambda_i}{2} \right) \frac{S}{2} + \frac{\gamma}{6} \frac{C\beta_0}{2} + \right. \\ & + \left. \frac{S_{bl}R}{I} \frac{3S\beta_0}{2} - \frac{\gamma}{2} \left(\frac{\theta}{3} - \lambda_i \right) \frac{S}{2} \right\} \sin 2\psi + \\ & + \left\{ \frac{S_{bl}R}{I} (S^2 + C^2) \right\} \cos 3\psi + \\ & + \left\{ 2 \frac{S_{bl}R}{I} SC \right\} \sin 3\psi \end{aligned} \quad (50)$$

The non-dimensional D_i component on the rotor hub (d_i) is calculated in exactly the same manner, using figure 5:

$$d_i = \frac{D_i R}{I \Omega^2} = f_T \cos \psi - f_R \sin \psi \quad (51)$$

Substitution of equations (45) and (47) gives for the average d_i (\bar{d}_i):

$$\begin{aligned} \bar{d}_i = & -\frac{\gamma S}{4} \left[\frac{\theta}{3} - \frac{\lambda_i}{2} \right] - \frac{\gamma S}{4} \left(\frac{\theta}{3} - \lambda_i \right) + \\ & -\frac{\gamma}{12} C \beta_0 + \frac{S_{bl}R}{I} \frac{S \beta_0}{2} \end{aligned} \quad (52)$$

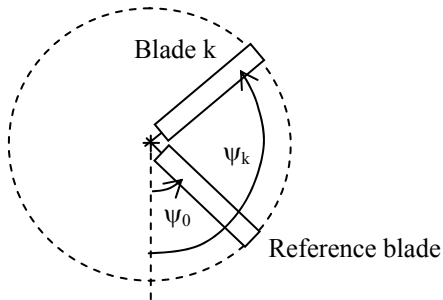


Fig. 6: Notations and symbols for the summation formulas.

And the fluctuating part (Δd_i) can be expressed as:

$$\begin{aligned} \Delta d_i = & \left\{ \frac{\gamma}{6} S^2 - \frac{\gamma}{2} \lambda_i \left(\frac{\theta}{2} - \lambda_i \right) - \frac{1}{6} \frac{\bar{C}_{Dp} \rho R^4 c}{I} \right\} \cos \psi + \\ & + \left\{ -\frac{\gamma}{2} \left(\frac{\theta}{3} - \frac{\lambda_i}{2} \right) \beta_0 - \frac{\gamma}{6} CS + \frac{S_{bl}R}{I} \right\} \sin \psi + \\ & + \left\{ \frac{\gamma}{2} \left(\frac{\theta}{3} - \frac{\lambda_i}{2} \right) \frac{S}{2} + \frac{\gamma}{6} \frac{C\beta_0}{2} + \right. \\ & + \left. \frac{S_{bl}R}{I} \frac{3S\beta_0}{2} - \frac{\gamma}{2} \left(\frac{\theta}{3} - \lambda_i \right) \frac{S}{2} \right\} \cos 2\psi + \\ & + \left\{ -\frac{\gamma}{2} \left(\frac{\theta}{3} - \frac{\lambda_i}{2} \right) \frac{C}{2} + \frac{\gamma}{6} \frac{\beta_0 S}{2} + \right. \\ & + \left. \frac{S_{bl}R}{I} \frac{3C\beta_0}{2} + \frac{\gamma}{2} \left(\frac{\theta}{3} - \lambda_i \right) \frac{C}{2} \right\} \sin 2\psi + \\ & + \left\{ \frac{S_{bl}R}{I} 2SC \right\} \cos 3\psi + \\ & + \left\{ \frac{S_{bl}R}{I} (S^2 - C^2) \right\} \sin 3\psi \end{aligned} \quad (53)$$

3.3 Summation formulas

So far, the effects of only one single rotor blade have been considered. This section will show how the forces and moments that are acting on the rotor hub can be calculated for a rotor with multiple blades. The obvious way to do this is to calculate the contribution of each blade to the force or moment separately, and to sum these contributions to arrive at a resulting force or moment. The notations and symbols necessary for the summation formulas are explained below and in figure 6.

In figure 6 ψ_0 is the azimuth angle of the reference blade, this azimuth angle will be used as the non-dimensional time. ψ_k is the azimuth angle of the k^{th} blade, and k ranges from:

$$k = 0, 1, \dots, N-1 \quad (54)$$

where N is the number of blades of the rotor. The relation between ψ_0 en ψ_k is given by:

$$\psi_k = \psi_0 + k \frac{2\pi}{N} = \psi_0 + k \Delta \psi \quad (55)$$

The expressions for the forces and moments that have been developed in the previous sections are valid for each rotorblade. In order to be able to use them for the summation, in each equation

ψ has to be replaced by ψ_k , and C and S have to be replaced by C_k and S_k . Additionally, the summation of the different contributions of the different blades, has to be performed at the same point in time. Therefore it is necessary to rewrite all expressions to the non-dimensional time ψ_0 .

It is emphasized that contrary to the case of the conventional helicopter, the coefficients C_k and S_k are not the same for the different blades. This is because in the Ornicopter configuration the different blades no longer have the same tip path plane.

To clarify the explanation given above, a general example is given of the summation formula for a force:

$$F = C \cos n\psi + S \sin n\psi \quad (56)$$

$$\sum F = \sum_{k=0}^{N-1} C_k \cos n\psi_k + S_k \sin n\psi_k \quad (57)$$

$$\begin{aligned} \sum F = \sum_{k=0}^{N-1} C_k \cos(n\psi_0 + nk\Delta\psi) \\ + S_k \sin(n\psi_0 + nk\Delta\psi) \end{aligned} \quad (58)$$

When the coefficients C_k and S_k are known, as well as the number of blades and the difference in azimuth angle between the blades, equation (58) gives the summation formula to calculate the forces (or moments) that act on the rotor hub as a result of multiple rotor blades.

4 Configuration analysis based on vibrations

For a feasible Ornicopter concept all the average values of the forces and moments on the rotor hub caused by the entire rotor need to equal zero (except for the vertical force). By choosing an appropriate number of blades and an appropriate flapping sequence of the blades these average values can indeed be reduced to zero. In this section three different Ornicopter configurations will be analyzed. Once the average values of these configurations are proven to be equal to zero, the fluctuating parts of the forces and moments about the rotor hub will be calculated.

And finally, the configuration that causes the least vibrations will be identified.

4.1 Double teeter configuration

The double teeter configuration has been chosen as a concept because of the relative simplicity of its forced flapping mechanism. The principle of the double teeter configuration is depicted in figure 7. As indicated by its name, the rotor consists of two teeters: the two opposite blades are connected like a see-saw, which means that if one blade is flapping upwards, the opposite blade is flapping downwards. All four of the blades are forced to flap with a 1-P frequency. At the moment in time that one of the two teeters is at its maximum flapping angle, the other teeter will be in the neutral position, as shown in figure 7. The tip path planes of the two teeters are anti-symmetrically tilted with respect to the shaft.

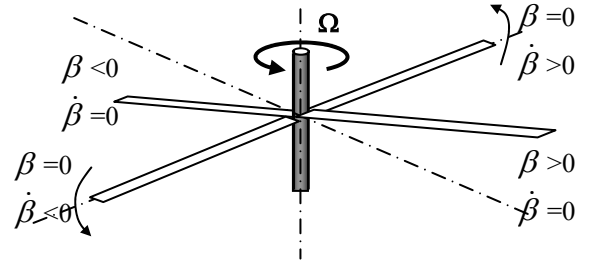


Fig. 7: Principle of the four bladed double teeter rotor.

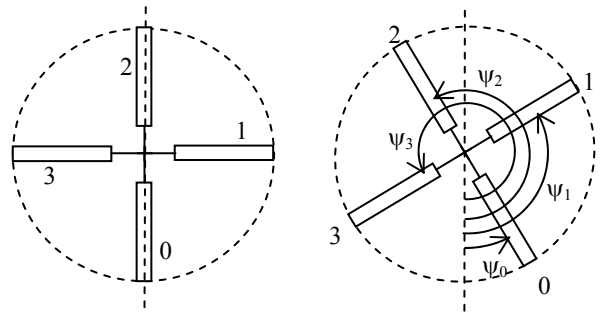


Fig. 8: Definition of the rotor blades $k=0, 1, 2, 3$

As can be seen from figure 7 the following holds for the number of blades and the difference in azimuth angle:

$$N = 4 \text{ and } \Delta\psi = \frac{\pi}{2} \quad (59)$$

The blades are numbered as indicated in figure 8. Now assume that the tip path plane of blade $k=0$ is described by the following expression:

$$\beta = C_0 \cos \psi_0 + S_0 \sin \psi_0 \quad (60)$$

If S_0 is chosen to be zero C_0 can be calculated using equation (23) (since in this case $\beta_{\max} = C_0$):

$$S_0 = 0 \text{ and } C_0 = \frac{8}{\gamma} m_{fl \max} \quad (61)$$

Using figures 7 and 8, the coefficients for the other blades ($k=1,2,3$) can now be derived as well. Since the tip path plane of blades $k=0$ and $k=2$ are equal, the coefficients of the flapping angle will also be the same for both blades:

$$C_2 = C_0 \text{ and } S_2 = S_0 = 0 \quad (62)$$

The other two blades ($k=1$ and $k=3$) share the same tip path plane as well, however they rotate in a different tip path plane than blades $k=0$ and $k=2$. At the azimuth angle at which blades $k=0$ and $k=2$ are at their highest point ($\psi=0$), at that same azimuth angle blades $k=1$ and $k=3$ will be at their lowest point (see figure 7), hence:

$$C_1 = -C_0 \text{ and } S_1 = 0 \quad (63)$$

$$C_3 = -C_0 \text{ and } S_3 = 0 \quad (64)$$

The above results in the following flapping equations for each of the blades:

$$\beta_0 = C_0 \cos \psi_0 \quad (65)$$

$$\beta_1 = -C_0 \cos \psi_1 \quad (66)$$

$$\beta_2 = C_0 \cos \psi_2 \quad (67)$$

$$\beta_3 = -C_0 \cos \psi_3 \quad (68)$$

Now the flapping equations for all four rotor blades are known, it is possible to calculate the forces and moments that this configuration causes about the rotor hub. Substituting the coefficients into the equations in paragraph 3.2 and using the summation formulas as given in

3.3 yields the total forces and moments due to all four rotor blades. As an example:

$$\begin{aligned} \sum m_r = & \sum_{k=0}^3 -\frac{\gamma}{16} C_k + \\ & + \frac{\gamma}{16} (S_k \sin 2(\psi_0 + k\Delta\psi) + C_k \cos 2(\psi_0 + k\Delta\psi)) \end{aligned} \quad (69)$$

$$\sum m_r = \frac{\gamma}{4} C_0 \cos 2\psi_0 \quad (70)$$

Some calculation now yields:

$$\sum m_p = \frac{\gamma}{4} C_0 \sin 2\psi_0 \quad (71)$$

$$\sum \Delta q = 0 \quad (72)$$

$$\sum \Delta v = 0 \quad (73)$$

$$\sum \bar{h}_i = 0 \quad (74)$$

$$\begin{aligned} \sum \Delta h_i = & \left(\frac{\gamma \lambda_i}{2} + \frac{S_{bl} R}{I} 6\beta_0 \right) C_0 \cos 2\psi_0 + \\ & + \frac{\gamma \beta_0}{3} C_0 \sin 2\psi_0 \end{aligned} \quad (75)$$

$$\sum \bar{d}_i = 0 \quad (76)$$

$$\begin{aligned} \sum d_i = & \frac{\gamma \beta_0}{3} C_0 \cos 2\psi_0 + \\ & - \left(\frac{S_{bl} R}{I} 6\beta_0 + \frac{\gamma \lambda_i}{2} \right) C_0 \sin 2\psi_0 \end{aligned} \quad (77)$$

4.2 2x2 anti-symmetrical configuration

Although the forced flapping mechanism of the 2x2 anti-symmetrical configuration will be more complicated than that of the double teeter configuration, this configuration is considered because of its expected favorable vibration characteristics. The rotor in anti-symmetrical configuration consists of four blades as well, but now the two opposite blades are flapping in the same direction. So (looking at figure 9) if blade $k=0$ is flapping upwards, blade $k=2$ is flapping

upwards as well, while at the same time the two other blades will be flapping downwards, and vice versa. The blades will pass through the neutral position at the same moment in time.

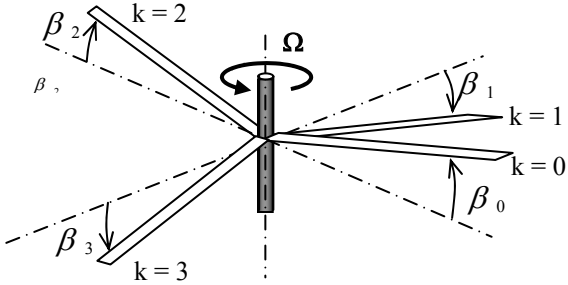


Fig. 9: Principle of the 2x2 anti-symmetrical rotor.

For the anti-symmetrical configuration the following expressions hold:

$$N = 4 \text{ and } \Delta\psi = \frac{\pi}{2} \quad (78)$$

Again, assume that the tip path plane of blade $k=0$ is described by equation (60) S_0 is chosen equal to zero, and C_0 is given by (61).

When looking at figure 9, it can be seen that blade $k=2$ is rotating in a different tip path plane than blade $k=0$. At the azimuth angle at which blade $k=0$ is at its highest point ($\psi=0$), at that same azimuth angle, blade $k=2$ will be at its lowest point. This tip path plane can be described by the following coefficients:

$$C_2 = -C_0 \text{ and } S_2 = S_0 = 0 \quad (79)$$

Blade $k=3$ is rotating in a different tip path plane as well. At the azimuth angle at which blade $k=0$ is at its highest point ($\psi=0$), at that same azimuth angle blade $k=3$ is at its neutral point and flapping upwards (see figure 9), so:

$$C_3 = 0 \text{ and } S_3 = C_0 \quad (80)$$

At the azimuth angle at which blade $k=0$ is at its highest point, blade $k=1$ is at its neutral point as well, but is flapping downwards:

$$C_1 = 0 \text{ and } S_1 = -C_0 \quad (81)$$

With the coefficients known, the resulting forces and moments about the rotor hub can again be calculated:

$$\sum m_r = 0 \quad (82)$$

$$\sum m_p = 0 \quad (83)$$

$$\sum \Delta q = 4C_0^2 \left(\sin 2\psi_0 + \frac{\gamma}{16} \cos 2\psi_0 \right) \quad (84)$$

$$\sum \Delta v = 0 \quad (85)$$

$$\sum \bar{h}_i = 0 \quad (86)$$

$$\sum \Delta h_i = 0 \quad (87)$$

$$\sum \bar{d}_i = 0 \quad (88)$$

$$\sum \Delta d_i = 0 \quad (89)$$

4.3 Three bladed 1-plane configuration

For this three bladed configuration the three blades are always in one plane although each blade rotates in a different tip path plane (see figure 10). This configuration is considered because of the simplicity of its forced flapping mechanism (consisting of a swash plate rotating at twice the rotation speed of the rotor [3]).

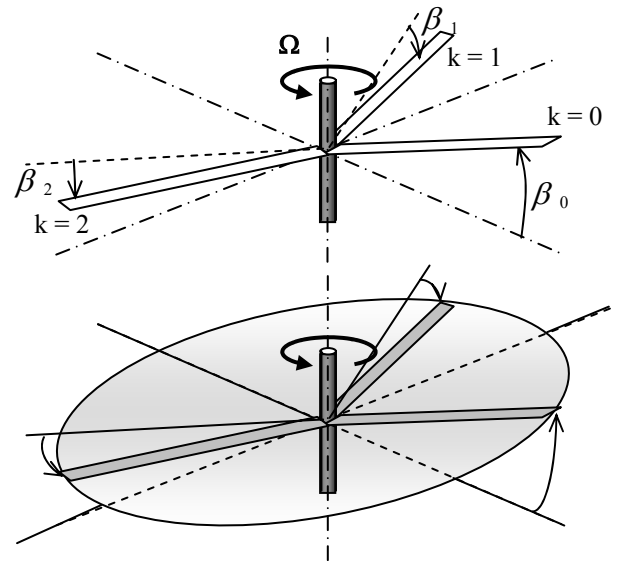


Fig. 10: Principle of the three bladed 1-plane rotor, blade $k=0$ is at its maximum flapping angle, blade $k=1$ is flapping upwards, blade $k=2$ is flapping downwards.

The number of blades and difference in azimuth angle are for this configuration given by:

$$N = 3 \text{ and } \Delta\psi = \frac{2\pi}{3} \quad (90)$$

Again, assume that the tip path plane of blade $k=0$ is described by equation (60). S_0 is chosen to be equal to zero, meaning that C_0 is given by (61). The movements of the other two blades ($k=1$ and $k=2$) for this configuration are described by the following flapping coefficients:

$$C_1 = -\frac{C_0}{2} \text{ and } S_1 = -\sqrt{\frac{3}{4}}C_0 \quad (91)$$

$$C_2 = -\frac{C_0}{2} \text{ and } S_2 = \sqrt{\frac{3}{4}}C_0 \quad (92)$$

The resulting forces and moments are given by:

$$\sum m_r = 3\frac{\gamma}{16}C_0 \cos 2\psi_0 \quad (93)$$

$$\sum m_p = -3\frac{\gamma}{16}C_0 \sin 2\psi_0 \quad (94)$$

$$\sum \Delta q = 0 \quad (95)$$

$$\sum \Delta v = 0 \quad (96)$$

$$\sum \bar{h}_i = 0 \quad (97)$$

$$\begin{aligned} \sum \Delta h_i = & \frac{\gamma}{4}C_0^2 \sin \psi_0 + \frac{\gamma}{4}C_0\beta_0 \sin 2\psi_0 + \\ & + \frac{3}{2}C_0 \cos 2\psi_0 \left(\frac{\gamma\lambda_i}{4} + 3\beta_0 \frac{S_{bl}R}{I} \right) \end{aligned} \quad (98)$$

$$\sum \bar{d}_i = 0 \quad (99)$$

$$\begin{aligned} \sum \Delta d_i = & -\frac{\gamma}{4}C_0^2 \cos \psi_0 + \frac{\gamma}{4}C_0\beta_0 \cos 2\psi_0 + \\ & + \frac{3}{2}C_0 \sin 2\psi_0 \left(-\frac{\gamma\lambda_i}{4} - 3\beta_0 \frac{S_{bl}R}{I} \right) \end{aligned} \quad (100)$$

4.4 Comparison of the different configurations

Considering the facts that a 2-P vibration is easier to damp than a 1-P vibration, that a torque fluctuation is easier to damp than a vibration in roll or pitch direction, and taking the order of the magnitude of the vibration into account, it is concluded that the 2x2 anti-symmetrical configuration is the best choice from a vibrations point of view. Especially since the torque vibration that is present is not an uncommon vibration, it also occurs in single teeter helicopters.

5 Conclusions

Expressions have been derived for the mechanical flapping moment, the flapping angle and the mechanical flapping power. Subsequently expressions for all six dynamic fluctuating force and moment components as these are caused by one rotor blade on the rotor hub have been derived. These expressions can be used to calculate the forces and moments that are caused on the rotor hub by the entire rotor.

Using these expressions three different Ornicopter configurations have been analyzed. Whereas all three Ornicopter configurations satisfy the requirement that the average forces and moments about the rotor hub have to be equal to zero, the vibrations that result for each configuration differ considerably. It can be concluded that the 2x2 anti-symmetrical configuration is the most favorable configuration from a vibration point of view.

6 References

- [1] Holten Th van. A single rotor without reaction torque: a violation of Newton's Laws or feasible?, *Proceedings of the 28th European Rotorcraft Forum*, Bristol, United Kingdom, September 2002
- [2] Holten Theo van, Heiligers Monique, Waal Gerard-Jan van de. The Ornicopter: a single rotor without reaction torque, basic principles, 24th *ICAS Congress*, Yokohama, Japan, August-September 2004
- [3] Waal GJR van de. *Development and Testing of the Ornicopter Wind Tunnel Model, Thesis Report*, Delft University of Technology, Faculty of Aerospace Engineering, 2003.